IOPscience iopscience.iop.org

Home Search Collections Journals About Contact us My IOPscience

The origin of preferred orientation during carbon film growth

This article has been downloaded from IOPscience. Please scroll down to see the full text article.

2009 J. Phys.: Condens. Matter 21 225003

(http://iopscience.iop.org/0953-8984/21/22/225003)

View the table of contents for this issue, or go to the journal homepage for more

Download details:
IP Address: 129.252.86.83
The article was downloaded on 29/05/2010 at 20:04

Please note that terms and conditions apply.

IOP Publishing — Journal of Physics: Condensed Matter
J. Phys.: Condens. Matter **21** (2009) 225003 (9pp) doi:10.1088/0953-8984/21/22/225003

The origin of preferred orientation during carbon film growth

M B Taylor[1], D W M Lau[1], J G Partridge[1], D G McCulloch[1], N A Marks[2], E H T Teo[3] and D R McKenzie[4]

[1] Applied Physics, School of Applied Science, RMIT University, GPO Box 2476V, Melbourne, Victoria 3001, Australia
[2] Nanochemistry Research Institute, Curtin University of Technology, GPO Box U1987, Perth WA 6845, Australia
[3] School of Electrical and Electronic Engineering, Nanyang Technological University, 639798, Singapore
[4] Applied and Plasma Physics, School of Applied Physics (A28), University of Sydney, Sydney, New South Wales 2006, Australia

E-mail: matthew.taylor@rmit.edu.au

Received 23 December 2008, in final form 12 March 2009
Published 22 April 2009
Online at stacks.iop.org/JPhysCM/21/225003

Abstract
Carbon films were prepared using a filtered cathodic vacuum arc deposition system operated with a substrate bias varying linearly with time during growth. Ion energies were in the range between 95 and 620 eV. Alternating dark, high density (sp^3 rich) bands and light, low density (sp^2 rich) bands were observed using cross-sectional transmission electron microscopy, corresponding to abrupt transitions between materials with densities of approximately 3.1 and 2.6 g cm^{-3}. No intermediate densities were observed in the samples. The low density bands show strong preferred orientation with graphitic sheets aligned normal to the film. After annealing, the low density bands became more oriented and the thinner high density layers were converted to low density material. In molecular dynamics modelling of film growth, temperature activated structural rearrangements occurring over long timescales ($\gg$1 ps) caused the transition from sp^3 rich to oriented sp^2 rich structure. Once this oriented growth was initiated, the sputtering yield decreased and channelling was observed. However, we conclude that sputtering and channelling events, while they occur, are not the cause of the transition to the oriented structure.

1. Introduction

The properties of disordered or amorphous carbon (a-C) materials depend on the ratio of graphite-like (sp^2 hybridized) to diamond-like (sp^3 hybridized) bonds [1] and on the topology of the structure in three dimensions [2]. For example, when the material contains a majority of sp^3 bonds with the minority of sp^2 bonds randomly distributed, it is known as tetrahedral amorphous carbon (ta-C) [3] and is mechanically hard and electrically insulating. When the majority of bonds are sp^2, the material is relatively soft with moderate electrical conductivity. If the sp^2 component forms sheet-like structures with preferred orientation, the electrical conductivity approaches that of graphite in the direction parallel to the sheets [4]. The thermal conductivity of these sheet-like structures is also expected to be high since the graphene sheet has a high in-plane phonon velocity. These oriented structures could have applications as high conductivity anisotropic conductors in electronics [4]. The driving force behind the alignment of the graphitic sheets is not yet fully understood. One view is that it is caused by the minimization of elastic strain energy in response to an anisotropic stress field [3, 5] and another view is that it arises principally from dynamic processes such as selective sputtering or ion channelling [6].

When prepared as films by physical vapour deposition, ion energy, substrate temperature and post-deposition annealing are important factors in determining the microstructure of a-C. While preferred orientation is often observed in a-C films following annealing [7], it can also be induced in films grown at room temperature within a particular range of energies and intrinsic stresses [4, 8]. The optimal conditions are ion energies above 300 eV and stresses between 5 and 8 GPa [4]. In this

 © 2009 IOP Publishing Ltd Printed in the UK

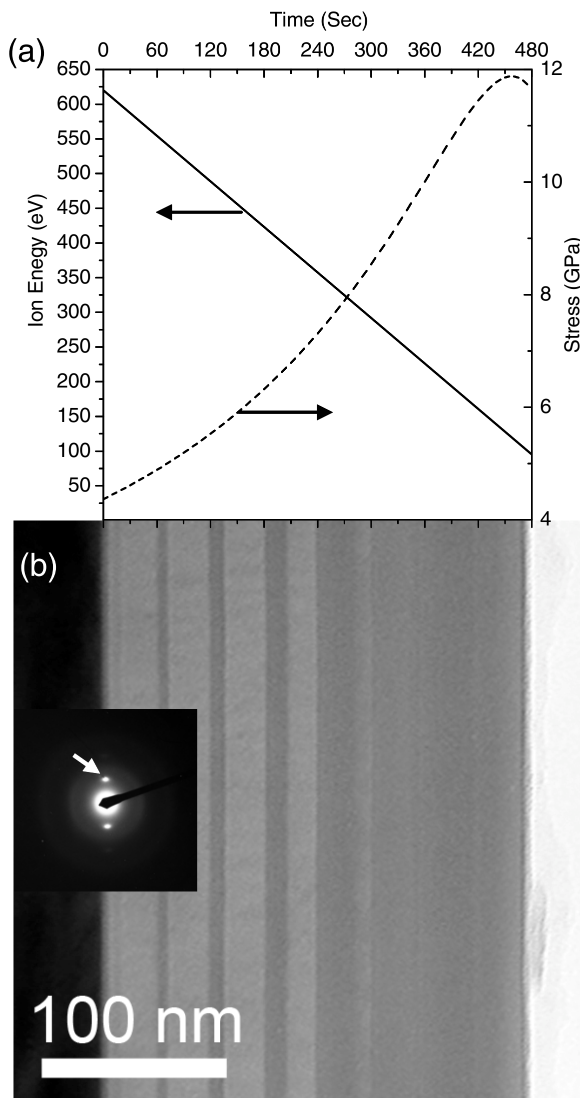

Figure 1. (a) The ion energy and the calculated stress as a function of deposition time for a film prepared with an applied substrate bias ramped between −600 and −75 V corresponding to average ion energies of 621 and 96 eV. The cross-sectional TEM image (b) contains bands corresponding to high density material (darker) and low density material (lighter). Inset in (b): a diffraction pattern showing strong {002} reflections (one of which is indicated by an arrow) from graphitic planes aligned perpendicular to the bands.

paper, we construct films with a built-in stress gradient and study their response to post-deposition annealing. By changing the ion energy as a function of time during deposition, the film stress is varied between conditions which favour oriented growth and those which favour high density ta-C. This creates, within a single sample, a continuous variation of growth conditions, leading to film properties that vary as a function of depth. Cross-sectional electron microscopy enabled the microstructure to be correlated with the deposition conditions. The thermal stability and stress relaxation processes were examined by performing post-deposition annealing. This allowed the effects of annealing on both oriented and non-oriented regions of the sample to be investigated. Molecular dynamics simulations of film growth were performed alongside

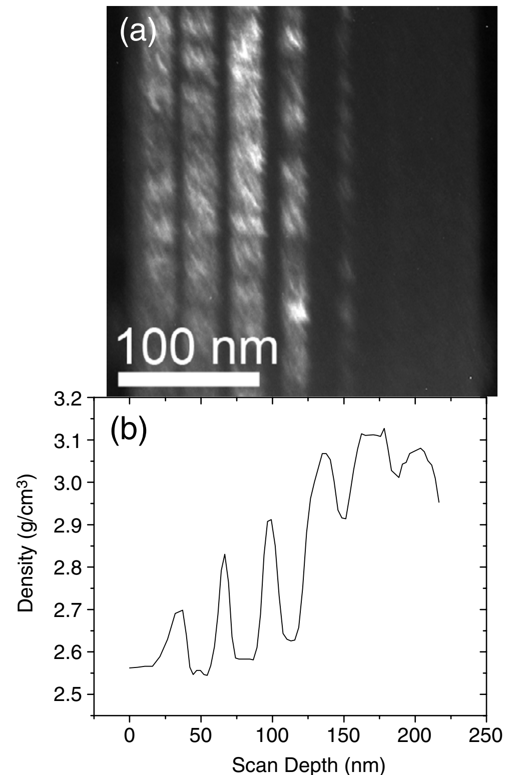

Figure 2. (a) Dark field cross-sectional TEM image of the film of figure 1(a) taken using a {002} graphitic reflection. (b) The density profile calculated from the plasmon energy as a function of distance from the substrate.

the experiments to suggest atomic scale mechanisms by which the oriented layers could form.

2. Methods

2.1. Material synthesis

Thin films of a-C were deposited onto p-type ⟨100⟩ silicon at room temperature using a flux of C ions generated from a dual-bend [9] filtered cathodic arc deposition system [10]. A 70 mm diameter, 99.999% pure graphite cathode was operated with an arc current of 56 A. The silicon substrates were placed in the deposition chamber which was pumped down to a base pressure of 6×10^{-6} Torr. The average ion energy was calculated from the plasma potential (measured to be 21 V using a Langmuir probe) and the substrate bias, assuming singly ionized carbon atoms [11]. The energy spread of the ions within the carbon plasma is estimated to be approximately 20 eV [12]. In order to determine the relationship between ion energy and stress, a series of films were fabricated at different ion energies. The thickness of each film and the radius of curvature of each silicon substrate were measured using a Tencor P-16 profiler and the intrinsic stress was calculated using Stoney's equation [13]. The radius of curvature of each silicon substrate was measured in two orthogonal directions to improve the accuracy of the derived stress. Films with an intentionally graded stress were synthesized using a PC interfaced programmable voltage

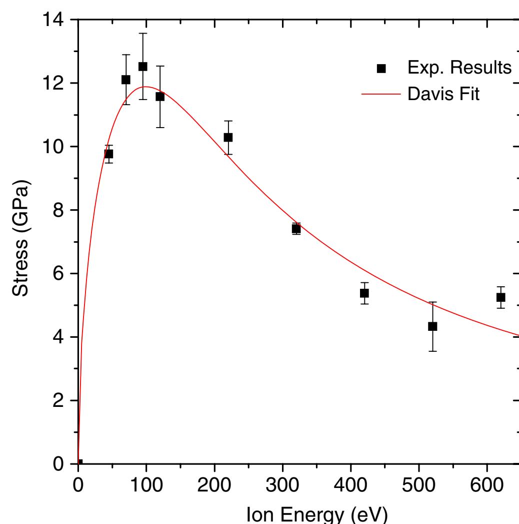

Figure 3. Stress as a function of ion energy for a series of single layer films prepared at constant ion energy. The line shows the fit to the data using the Davis [19] model with fitting parameters of $k = 0.0002$, $K = 1.7$ (see text).

(This figure is in colour only in the electronic version)

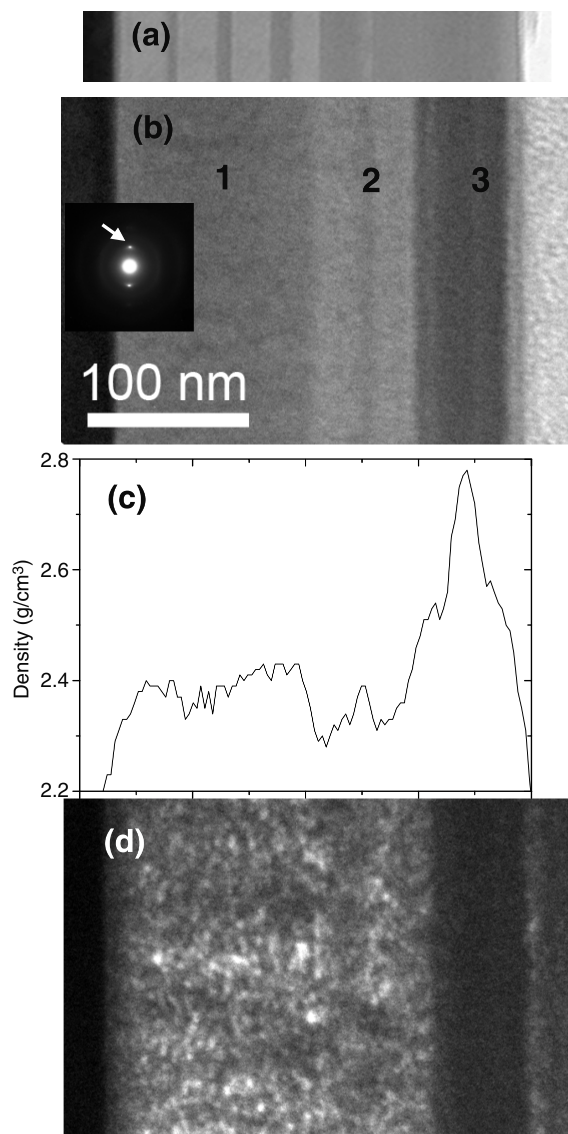

Figure 4. (a) Bright field cross-sectional TEM image of the film shown in figure 1(a); (b) the same film after annealing at 600 °C (inset: selected area diffraction pattern); (c) the density profile and (d) the dark field image taken from a {002} reflection (indicated by an arrow in (b)).

source to control the substrate bias during film growth. All films were prepared with a 60 s break after every 60 s of deposition in order to reduce cathode heating. The rise in the substrate surface temperature caused by the deposition process was measured *in situ* using a thermocouple and was found to be approximately 30 °C for a sample biased at −75 V and approximately 40 °C for a sample biased at −600 V.

2.2. Microstructural characterization

Transmission electron microscopy (TEM) and electron energy loss spectroscopy (EELS) were used to investigate the microstructure, density and bonding configurations in the carbon films. Cross-sectional specimens were prepared by mechanical polishing followed by ion bean thinning (4 keV Ar ions at 4° incident angle). Scanning TEM, with a probe size of approximately 5 nm, was used to obtain EELS line scans as a function of thickness. By measuring the plasmon energy in the low loss regime of the energy loss spectrum, the density of the material was calculated assuming a free-electron model with an effective mass of 0.88 times that of a free electron and 4 valence electrons per carbon atom [14, 15].

2.3. Theoretical modelling

Molecular dynamics (MD) simulations of carbon thin film growth were performed using the environment dependent interaction potential for carbon [16]. Films were grown using 40 or 70 eV mono-energetic carbon beams, in which five hundred atoms were introduced singly onto a pre-existing ta-C substrate. The motion associated with each impact was followed for approximately one picosecond. Prior to each impact, the entire system was heated for times between 0.25 and 1 ps at temperatures between 1000 and 2500 K. The time for which the elevated temperature is maintained is the activation time, t_{act} and the temperature to which the system is heated is the activation temperature, T_{act}. This temperature-pulsing method [17] activates infrequent atomic processes (sometimes referred to as *rare events*), which are overlooked in traditional MD simulations of thin film growth. For further details see [18]. After each pulse, any atoms not connected to the main system were considered to be 'sputtered' and were removed from the simulation.

Due to computational constraints, it was not possible to simulate the same range of energies as used in the experiment. Instead, we take advantage of the coupling between the substrate temperature and the energy of the incident species. For example, it has been shown experimentally [4] that the transition in carbon films between an sp^3-rich phase and an sp^2-rich phase occurs at a well defined ion energy, as the ion energy

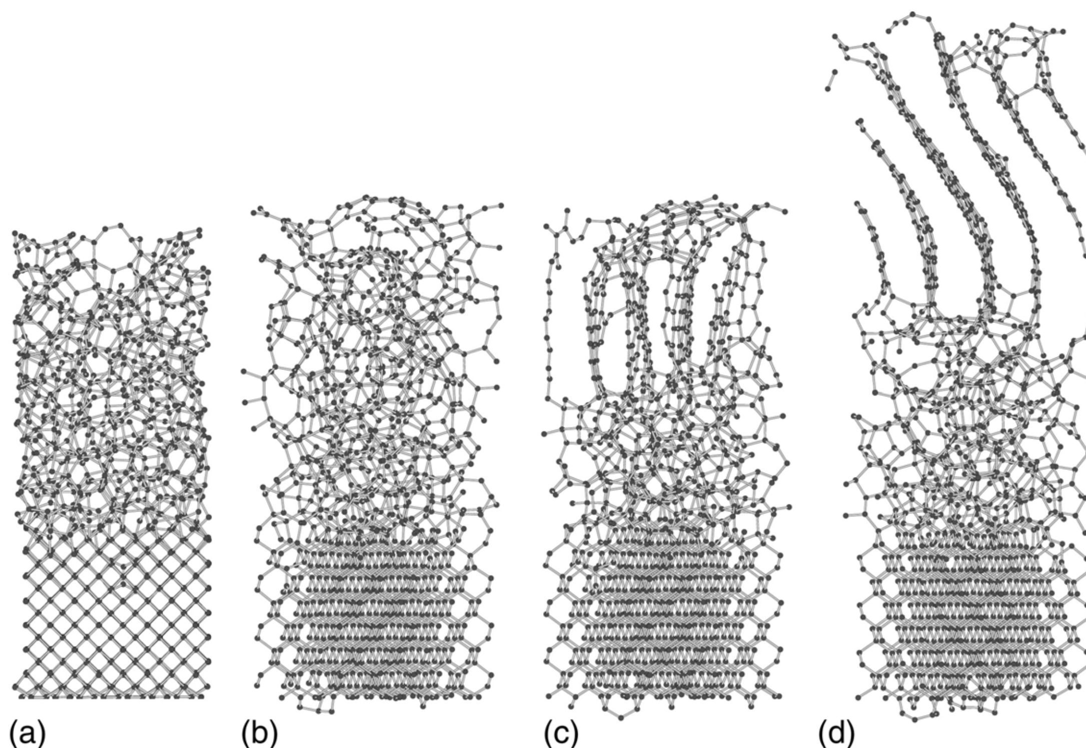

Figure 5. Snapshots of a simulation in which 40 eV atoms are deposited onto a ta-C substrate. Infrequent events are activated using the parameters $T_{act} = 2000$ K and $t_{act} = 1$ ps. (a) The initial substrate, consisting of ta-C attached to diamond; (b) after 120 atoms have been deposited; (c) after 200 atoms have been deposited (oriented growth commences around the 160 atom mark); (d) the final structure (500 atoms deposited).

is increased. The energy at which this transition occurs can be lowered by increasing the substrate temperature, showing that the structural effects of increased temperature mimic those of increased ion energy. In our simulations, we increase the 'effective energy' of the incident ions by increasing T_{act}.

To quantify the amount of orientation in each simulation, we define an orientation parameter by analogy with materials texture analysis. Each sp^2-bonded atom in the film is used to define a set of normal vectors which are projected onto a unit sphere. The degree of orientation was determined by applying histogram binning over the sphere followed by a surface density analysis. The order parameter is defined such that a value close to unity corresponds to a uniform distribution of points over the sphere, indicating randomly oriented sp^2 bonds. Large positive values reflect clustering of the normal vectors on the unit sphere and indicate highly oriented sp^2 networks.

3. Results and discussion

3.1. The microstructure of the films

Figure 1(a) shows the ion energy as a function of deposition time for a film synthesized using a linear substrate bias ramp from −600 to −75 V, resulting in average ion energies ranging from 621 to 96 eV during growth. The bright field cross-sectional TEM image of this sample is shown in figure 1(b) and exhibits significant contrast variation through the thickness of the film, with clearly defined light and dark bands running parallel to the surface of the substrate. The top of each light band coincides with each 60 s break in the deposition. The diffraction pattern taken from this film (inset in figure 1(b)) shows well defined graphitic {002} reflections from graphitic planes aligned perpendicular to the bands.

Figure 2(a) shows a dark field image formed using one of the {002} reflections from the same area of the sample as shown in figure 1(b). The dark field image reveals that the light bands in figure 1(b) are composed of oriented regions which extend across each band. Figure 2(b) shows the density as a function of distance from the substrate. The density profile shows repeated abrupt changes from ∼2.5 g cm^{-3} in the oriented (bright) bands to ∼3.1 g cm^{-3} in the dark bands. A value of 3.1 g cm^{-3} indicates that the dark bands are composed of ta-C. In areas where the width of a band is comparable to the probe size (5 nm), there are contributions from both high and low density bands. Therefore, the density values obtained from thin ta-C and thin oriented graphitic bands are respectively lower and higher than those obtained from thick bands.

In previous work [4], ion energy and stress were found to be the critical parameters that determine whether or not oriented graphitic carbon films are formed. In order to estimate the stress for a given ion energy, we fitted the model of Davis *et al* [19] to the stress measured from a set of carbon films prepared with a range of constant ion energies [4]. Figure 3 shows the stress versus ion energy for these films along with the fit to the data using the model with fitting parameters of $k = 0.0002$, $K = 1.7$. Using these parameters, figure 1(a) shows the stress calculated from the ion energy during the

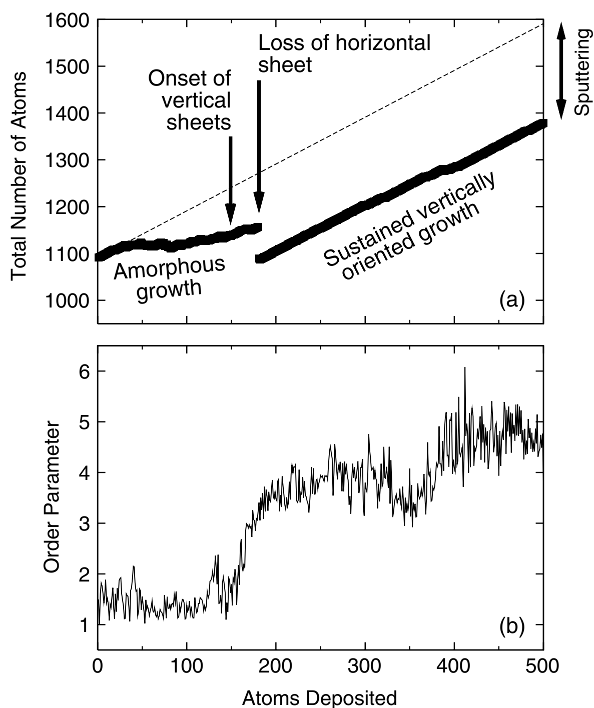

Figure 6. Time evolution of the 40 eV simulated deposition shown in figure 5. (a) The number of atoms present in the simulation as a function of the number of atoms deposited. The labels and arrows indicate critical stages in the growth. The dashed line indicates the increase in deposited atoms without sputtering. (b) Variation in the order parameter (see text for definition) as a function of the number of atoms deposited. The onset of vertical ordering is apparent in the sharp rise in order after 160 atoms have been deposited.

deposition of the film shown in figure 1(b). The oriented graphitic bands only form when the ion energy is greater than 280 eV and when the stress lies between ~4.5 and ~7.5 GPa, in agreement with previous work [4].

We now explain the microstructure shown in figure 1(b) in terms of the stress conditions shown in figure 1(a). During the initial stages of film growth, where the average ion energy was 620 eV and the stress was ~4.5 GPa, oriented graphitic carbon formed adjacent to the silicon substrate. The oriented phase continued to grow until the first interruption after 60 s of deposition. This layer appears as the first light band, approximately 30 nm in thickness, visible in the TEM image (figure 1(b)). Upon continuing the deposition, a thin band of ta-C was formed initially before growth reverted to the oriented graphitic phase. Following each subsequent interruption, progressively thicker ta-C bands were produced until no oriented graphitic bands were formed. With increasing deposition time, the stress increases (as the ion energy decreases) and the deposition conditions increasingly favour ta-C. The mechanism which promotes the growth of ta-C after each interruption and the switch to the oriented graphitic phase was investigated with molecular dynamics modelling and is described below.

The sample in figure 1(b) was annealed for 10 min at 600 °C and the resulting microstructure is shown in figure 4(b). For comparison, a portion of the non-annealed sample (figure 1(b)) is shown in figure 4(a). Annealing significantly alters the microstructure, leading to the disappearance of the narrow ta-C bands and reconstruction of the film into three main regions (labelled 1 to 3 in figure 4(b)). A quantitative measure of the effect of annealing on the degree of alignment of the graphitic sheets within the film was obtained by measuring the change in angular spread of the {002} diffraction arcs. This angular spread reduction was 50%, indicating a significant increase in the degree of alignment of the graphitic sheets.

The density profile and dark field image (taken from a graphitic {002} reflection from this sample) are shown in figures 4(c) and (d) respectively. The dark field image reveals that region 1 contains oriented graphitic material, whilst the density profile reveals that it is of uniform density. The annealing has transformed the first three narrow ta-C bands within region 1 (figure 4(a)) into a single low density oriented graphitic layer. The density profile shows that the microstructure in region 2 consists of two distinct low density layers, which before annealing were high density layers. Finally, the largely high density layer (band 3) has been retained at the surface of the film.

The structural transformations which occurred in this film after annealing can be understood as follows. The thin, ta-C bands in region 1 transform to the sp^2 structure since they are under the least compressive stress (compressive stress helps to stabilize the ta-C structure) and are surrounded on both sides by oriented material which acts as a template for the transformation. As the thin ta-C bands in region 1 transform to lower density oriented material, they expand and in so doing reduce the compressive stress acting on region 2.

Region 3 contains the thickest continuous region of ta-C and is therefore not subjected to strong templating. In this region, the ta-C can reduce its stress without substantially changing its structure, as previously observed [20]. In region 2, sp^2 material of lower density than that in region 1 has formed (see figure 4(c)), possibly because of the sequencing of the transformation. If layers in region 1 and region 2 transform at different times, they will do so under different stress conditions and so develop different microstructures.

3.2. Modelling

The goal of our simulations was to provide atomic-level insight into the main structural characteristics of figures 1 and 2; namely the light and dark bands, the rarity of films with intermediate densities, and the abrupt nature of the transformation from amorphous to vertical orientation. Figure 5 shows the appearance of preferred orientation during the simulated growth of a carbon film at 40 eV using temperature pulsing (T_{act} = 2000 K, t_{act} = 1 ps) to activate infrequent events. In the oriented phase, sp^2 atoms are arranged in vertical graphitic sheets. The oriented growth does not appear immediately, as indicated by the snapshot after 120 atoms have been deposited (figure 5(b)). However, the growth mode switches after approximately 160 atoms have been deposited (figure 5(c)) and all subsequent growth continues in the oriented mode. This delayed onset of the oriented

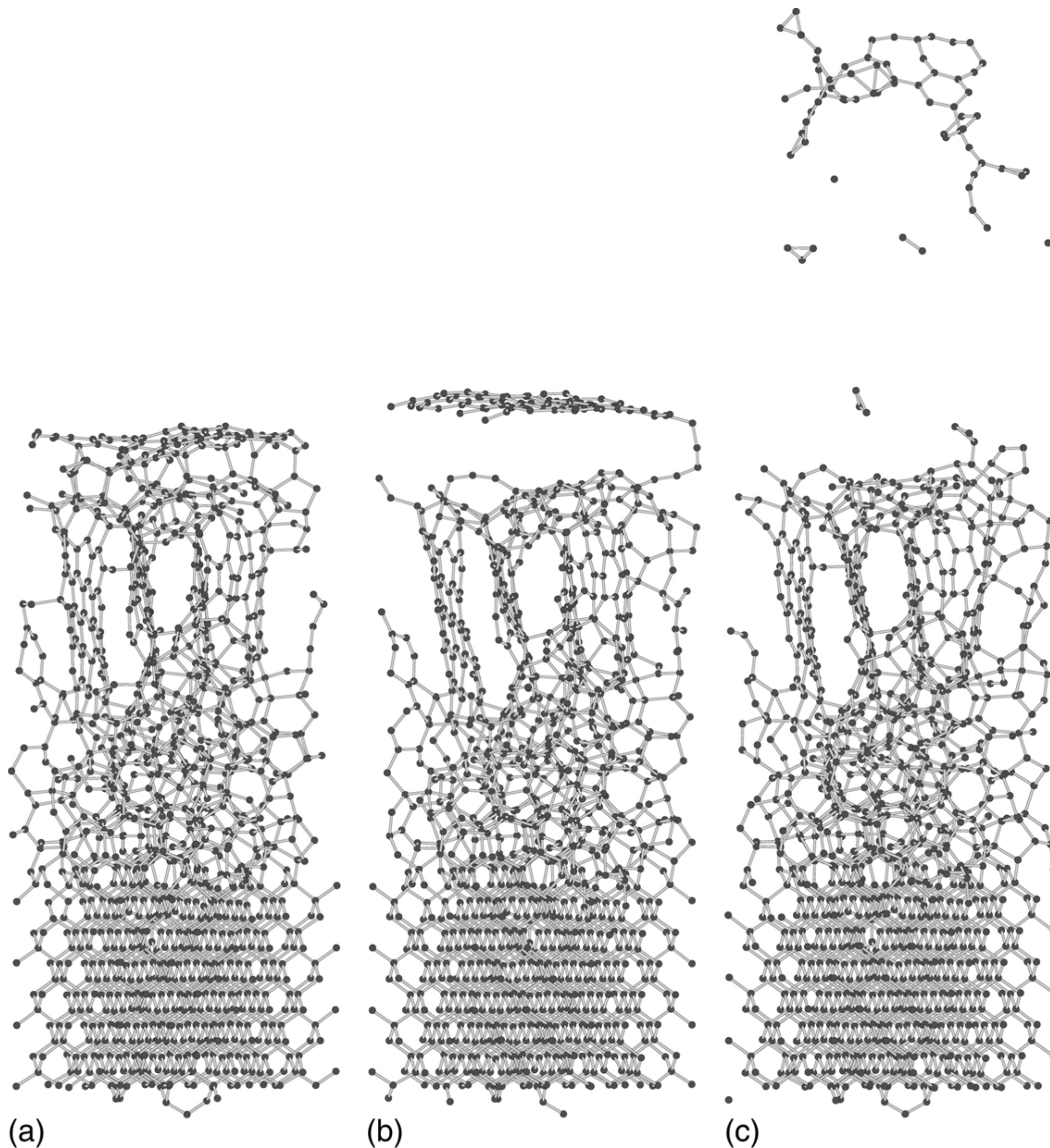

Figure 7. Successive snapshots at the conclusion of the temperature-pulsing sequence for the 40 eV deposition shown in figures 5 and 6. (a) After 178 atoms have been deposited; (b) after 179 atoms have been deposited, showing a highly ordered horizontal graphitic layer; (c) after 180 atoms have been deposited, showing the horizontal sheet has been sputtered away (see transition noted in figure 6).

growth mode is also observed in the experimental results of figure 1(b), where dark bands appear after each interruption to the deposition process. In light of the simulations, our interpretation is that a thin sp^2 rich layer forms as a reconstruction of the surface when the deposition is paused. This reconstruction of the surface has also been observed experimentally [21]. When the deposition recommences, the growth mode is ta-C initially, subsequently switching to the vertically ordered sp^2 phase. In the simulations, this effect is also observed. At first, the simulated growth is ta-C but after a while the oriented phase appears and all subsequent growth continues in this manner.

To quantify the appearance of oriented growth in figure 5, we plot in figure 6(a) the number of atoms in the simulation versus the number of atoms deposited. Two distinct regimes are visible. Prior to the establishment of the oriented phase, amorphous growth occurs, accompanied by significant sputtering. After 160 atoms have been deposited (indicated by the left-hand arrow in figure 6(a)), vertical sheets appear within the upper layers of the film. After another 20 atoms have been deposited, the growth mode changes abruptly. Further growth consists entirely of vertically oriented sheets and sputtering occurs much less frequently. The appearance of order within the growing film is illustrated by the rapid increase in the order parameter shown in figure 6(b). This sequence of events is typical of all depositions where oriented growth was observed. In some simulations, including the example presented in figure 6, horizontal sheets are formed prior to the change in the growth mode. These structures are transient, and are readily broken up by the impacting energetic atoms. This process is shown in figure 7 in which two successive impacts

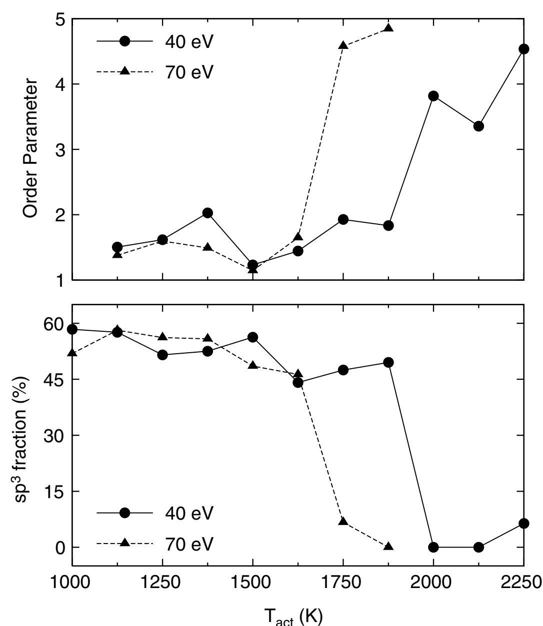

Figure 8. Order parameter and sp^3 fraction as a function of the activation temperature T_{act}. Results are reported for two different deposition energies, 40 eV (circles) and 70 eV (triangles). An increase in the simulated deposition energy decreases the critical temperature for ordered sp^2 phases, as in the experiment [20].

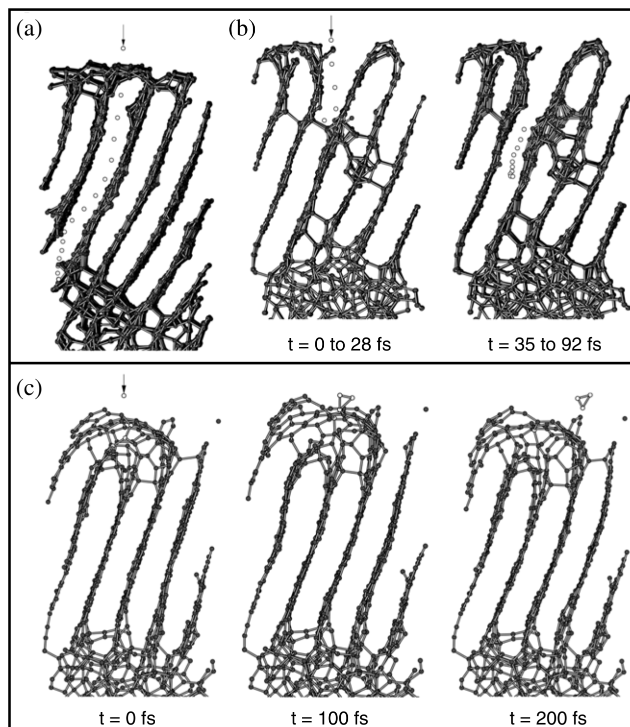

Figure 9. Molecular dynamics snapshots of typical impact phenomena following the nucleation of the oriented phase. All images are for 70 eV impacts, with the initial position in each impact indicated by an arrow. (a) A channelling process in which the incoming atom eventually lodges at the interface between the oriented and amorphous regions; (b) a knock-on process in which the incoming atom removes a bridging bond connecting adjacent graphitic sheets; (c) a sputtering process in which a small fragment (here a triangular unit displayed using white circles) is ejected from the surface following impact.

lead to the creation, and then the removal, of a horizontal graphitic sheet.

In figure 8, the sp^3 fraction and order parameter for a variety of activation temperatures have been plotted in order to verify that increased temperature can mimic the effects of increased ion energy. As discussed above and in previous work [17, 18], the horizontal axis is the computational analogue of the experimental substrate temperature. The difference in the specific value of the temperature at which the transition occurs (experimental critical temperatures are of order 450 K [22]) is due to the different timescales (picoseconds in the simulation versus milliseconds in the experiment). There is however a one-to-one correspondence between the value of T_{act} used in the simulation and the substrate temperature in the experiment via the Arrhenius relation. This correspondence enables the comparison of our data with the experimental work of Chhowalla *et al* [20], in which the critical temperature for 90 eV depositions was $\sim$50 K higher than for 130 eV depositions. In good qualitative agreement, a similar effect is seen in the simulations; the critical value of T_{act} is noticeably higher when a lower impact energy is used.

It is instructive to consider the dynamics of certain impacts and the resulting structural evolution of the film. Figure 9 shows molecular dynamics snapshots of typical impact phenomena occurring (at 70 eV) after the nucleation of the oriented phase. In figure 9(a), a channelling-like impact is shown in which the initial position of the impact species (denoted by the arrow) is such that the depositing atom bounces off the side-walls of the sp^2 sheets, eventually lodging at the interface between the amorphous and ordered regions. A similar event is shown in figure 9(b), with the distinction that, in this case, the starting configuration contains a bridging element connecting adjacent sheets. The deposition species has a ‘knock-out’ effect, which clears out any linking material, eventually lodging within one of the graphite-like walls. In the third class of impact (figure 9(c)), the surface structure is less amenable to channelling-like processes and the effect of the impact is to sputter a small triangular unit (highlighted using white circles).

The representative processes in figure 9 can be viewed in the light of previous explanations for oriented growth in which preferential sputtering or channelling [6] were proposed. However, the suggestion that sputtering or channelling can initiate the oriented structure is not supported by our simulations. Oriented structures are not seen at all except when rare events are activated. This is demonstrated in figure 10 which shows the effect of suppressing rare events by reducing the activation time t_{act}. For short activation times (figures 10(b), (c)), the deposition processes lead to amorphous material alone and oriented growth only occurs when the activation time is sufficiently long (figure 10(d)).

4. Conclusion

Carbon films were prepared with energies that changed progressively during deposition. Film growth was dominated

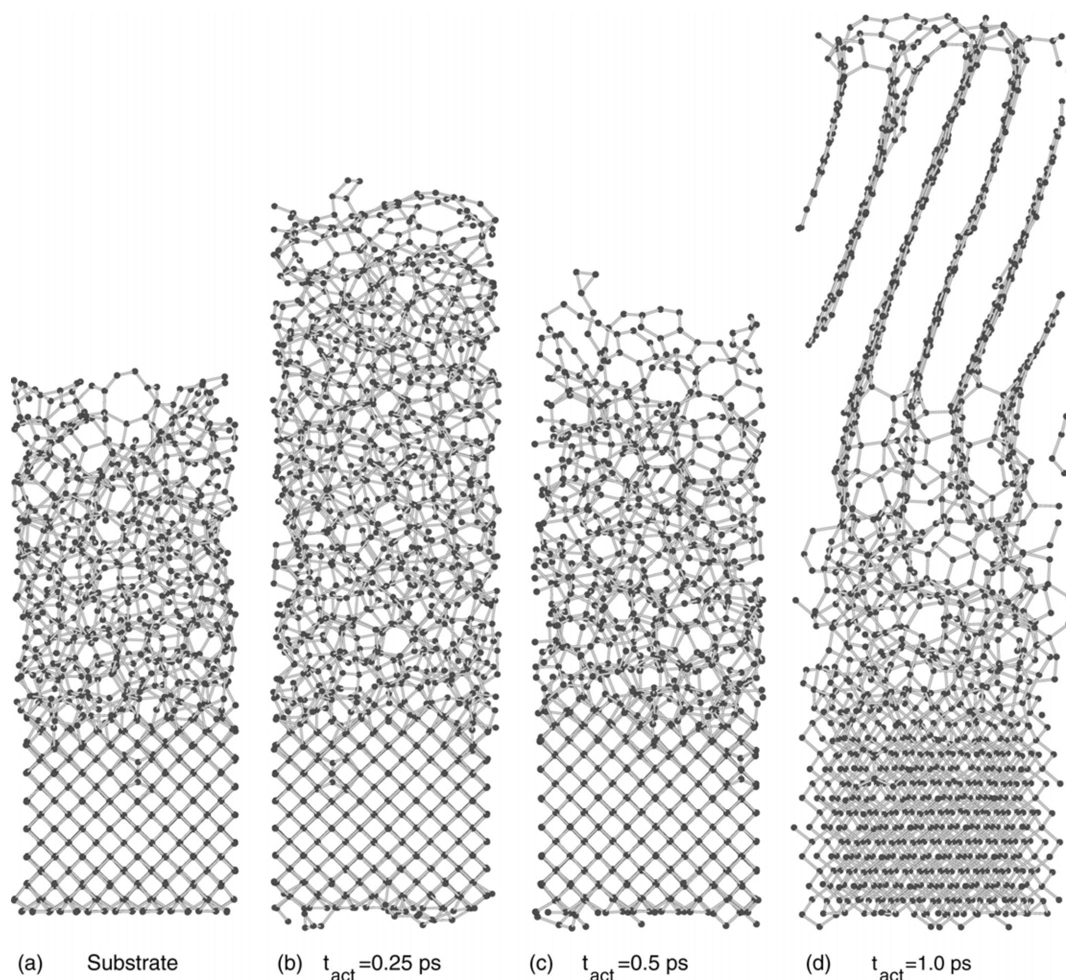

Figure 10. 70 eV deposition simulations with $T_{act} = 1875$ K illustrating the importance of the activation time t_{act}. (a) The initial ta-C substrate; (b) final structure after 500 atoms deposited using a very short activation time of 0.25 ps; (c) a repeat of (b) with $t_{act} = 0.5$ ps; (d) a repeat of (b) with $t_{act} = 1.0$ ps. Oriented growth is only observed with sufficient activation of rare events.

by two distinct structural forms with abrupt interfaces between them. These forms are a dense isotropic sp^3 rich structure and a highly oriented sp^2 rich material with vertically aligned graphitic sheets. Structures with intermediate density and sp^3 content did not occur. After annealing to 600 °C, some of the thinner sp^3 rich layers were converted into sp^2 rich material and the degree of preferred orientation increased. Atomistic modelling of carbon film growth showed that the transition is initiated by a temperature activated process. At the transition to oriented growth, strong channelling and a reduced sputter yield occur concurrently, but neither channelling nor sputtering cause the transition.

Acknowledgments

The authors would like to thank to Cenk Kocer for assistance in performing the molecular dynamics simulations. The authors also wish to acknowledge the financial support of the Australian Research Council.

References

[1] McKenzie D R 1996 *Rep. Prog. Phys.* **59** 1611–64
[2] Harris P J F 2005 *Crit. Rev. Solid State Mater. Sci.* **30** 235–53
[3] McKenzie D R, Muller D and Pailthorpe B A 1991 *Phys. Rev. Lett.* **67** 773–6
[4] Lau D W M, McCulloch D G, Taylor M B, Partridge J G, McKenzie D R, Marks N A, Teo E H T and Tay B K 2008 *Phys. Rev. Lett.* **100** 4
[5] Schwan J, Ulrich S, Theel T, Roth H, Ehrhardt H, Becker P and Silva S R P 1997 *J. Appl. Phys.* **82** 6024–30
[6] Lifshitz Y, Kasi S R and Rabalais J W 1989 *Phys. Rev. Lett.* **62** 1290
[7] McCulloch D G, Xiao X L, Peng J L, Ha P C T, McKenzie D R, Bilek M M M, Lau S P, Sheeja D and Tay B K 2005 *Surf. Coat. Technol.* **198** 217–22
[8] Ferrari A C, Libassi A, Tanner B K, Stolojan V, Yuan J, Brown L M, Rodil S E, Kleinsorge B and Robertson J 2000 *Phys. Rev.* B **62** 11089–103
[9] Shi X, Tay B K, Tan H S, Liu E, Shi J, Cheah L K and Jin X 1999 *Thin Solid Films* **345** 1–6
[10] Aksenov I I, Belous V A, Padalka V G and Khoroshikh V M 1978 *Sov. J. Plasma Phys.* **4** 425–8 (Engl. Transl.)
[11] Anders A 2002 *Vacuum* **67** 673–86
[12] Chhowalla M, Davis C A, Weiler M, Kleinsorge B and Amaratunga G A J 1996 *J. Appl. Phys.* **79** 2237–44
[13] Stoney G G 1909 *Proc. R. Soc.* A **82** 172–5
[14] Egerton R F 1996 *Electron Energy-Loss Spectroscopy in the Electron Microscope* 2nd edn (New York: Plenum)
[15] Titantah J T and Lamoen D 2004 *Phys. Rev.* B **70** 033101
[16] Marks N A 2001 *Phys. Rev.* B **63** 035401–7

[17] Marks N A, Cover M F and Kocer C 2006 *Appl. Phys. Lett.* **89** 131924
[18] Marks N A, Cover M F and Kocer C 2006 *Mol. Simul.* **32** 1271–7
[19] Davis C A 1993 *Thin Solid Films* **226** 30–4
[20] Chhowalla M, Yin Y, Amaratunga G A J, McKenzie D R and Frauenheim T 1996 *Appl. Phys. Lett.* **69** 2344–6
[21] McKenzie D R, Tarrant R N, Bilek M M M, Ha T, Zou J, McBride W E, Cockayne D J H, Fujisawa N, Swain M V, James N L, Woodard J C and McCulloch D G 2003 *Diamond Relat. Mater.* **12** 178–84
[22] Chhowalla M, Robertson J, Chen C W, Silva S R P, Davis C A, Amaratunga G A J and Milne W I 1997 *J. Appl. Phys.* **81** 139–45